TAJE_A_754793.3d (TAJE) 02-05-2013 23:56

Australian Journal of Earth Sciences (2013)
60, 217–229, http://dx.doi.org/10.1080/08120099.2012.754793

Towards a predictive model for opal exploration using a spatio-temporal data mining approach

A. S. MERDITH, T. C. W. LANDGREBE, A. DUTKIEWICZ* AND R. D. MÜLLER

EarthByte Group, School of Geosciences, The University of Sydney, NSW 2006, Australia.

Australia produces over 90% of the world's precious opal from highly weathered Cretaceous sedimentary rocks within the Great Artesian Basin. Since opal was first discovered around 1870 until the present day, opal mining has been carried out by private operators working a claim no larger than 50 × 50 m, usually in the direct vicinity of areas that have yielded precious opal in the past. Currently there is no formal exploration model for opal and its formation in the geological environment is poorly understood. Here we make the first systematic attempt to formulate a predictive model for opal exploration using a powerful data mining approach, which considers almost the entire Great Artesian Basin as a potential reservoir for precious opal. Our methodology uses all known locations where opal has been mined to date. Its formation and preservation in weathered Cretaceous host rocks is evaluated by a joint analysis of large digital data sets that include topography, regional geology, regolith and soil type, radiometric data and depositional environments through time. By combining these data sets as layers enabling spatio-temporal data mining using the GPlates PaleoGIS software, we produce the first opal prospectivity map for the Great Artesian Basin. Our approach reduces the entire area of the Great Artesian Basin to a mere 6% that is deemed to be prospective for opal exploration. It successfully identifies two known major opal fields (Mintabie and Lambina) that were not included as part of the classification dataset owing to lack of documentation regarding opal mine locations, and it significantly expands the prospective areas around known opal fields particularly in the vicinity of Coober Pedy in South Australia and in the northern and southern sectors of the Eromanga Basin in Queensland. The combined characteristics of these areas also provide a basis for future work aimed at improving our understanding of opal formation.

KEY WORDS: opal, Great Artesian Basin, data mining, data layering, prospectivity, mineral exploration, Cretaceous sedimentary rocks, Australian regolith.

Downloaded by [University of Sydney] at 15:42 05 September 2013

INTRODUCTION

Although Australia accounts for over 90% of the world's production of precious opal that is almost exclusively found within the Great Artesian Basin (Smallwood 1997), the mining community has been struggling over the past 20 years. This is, in part, the result of an aging and dwindling mining population comprising individual miners working on single 50 × 50 m or smaller claims under harsh conditions, the rising cost of mining necessities such as fuel and equipment imposed by the global economy and the fact that demand for precious opal is driven exclusively by its use as a decorative gem (opal is Australia's national gemstone) with no known industrial applications. Additionally, a critical factor in contributing to the decline in opal production is that no new significant opal discoveries have been made since the early 1900s (Barnes & Townsend 1990). As opal mining in Australia is largely a cottage industry, the majority of opal exploration simply occurs in the immediate vicinity of locations that have already yielded precious opal using traditional exploration techniques such as machine excavation and hand-held tools. Here we have used a systematic approach involving the investigation of associations between known opal localities in the Great Artesian Basin and particular features in a variety of open-access spatial geological and geophysical datasets, such as regolith and soil type and radiometric data that have a relationship with the occurrence of opal. By using data layering and feature extraction (Tan *et al.* 2006) from these digital datasets we have been able to tease out pertinent associations between opal locations and the data sets, and have translated them into an opal prospectivity map of the Great Artesian Basin, thus providing the first step towards predictive, systematic opal exploration.

GEOLOGICAL SETTING

Opal consists of amorphous $SiO_2.nH_2O$ comprising a network of silica spheres, which in precious opal are of similar size and form an ordered network allowing light to diffract into a spectacular array of colours (Sanders 1964). Precious opal is found in sedimentary and volcanic environments and is commonly referred to as

*Corresponding author. adriana.dutkiewicz@sydney.edu.au

© 2013 Geological Society of Australia

TAJE_A_754793.3d (TAJE) 02-05-2013 23:56

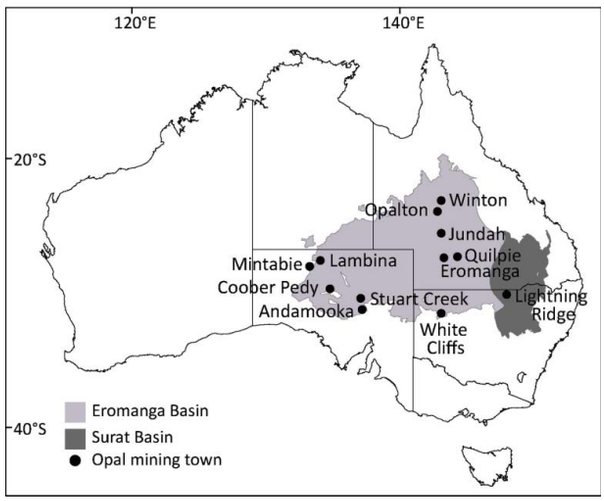

Figure 1 Map of Australia showing the extent of the Eromanga and Surat basins and the location of the major opal-producing townships. The Eromanga and Surat basins represent the southern eastern and western extents of the Great Artesian Basin.

'sedimentary opal' and 'volcanic opal.' Sedimentary opal is classified as opal-A and volcanic opal is classified as opal-CT based on X-ray diffraction analysis although other major differences include the degree of crystallinity, water content and density (Smallwood *et al.* 2008). Virtually all opal mined in Australia is sedimentary opal-A, which is thought to have formed from enriched silica solutions derived from the chemical weathering of feldspars in the host sequence (Smallwood *et al.* 2008). In Australia, sedimentary opal is found within fractures and primary and secondary pore spaces in the top 30 m (Barnes & Townsend 1990) of heavily weathered Cretaceous sedimentary rocks within the Eromanga and Surat basins that together comprise a significant portion of the Great Artesian Basin (Figure 1). The stratigraphy of Eromanga and Surat basins is dominated by alternating layers of sandstones, claystones and siltstones that were deposited *ca* 125 Ma to 95 Ma as a consequence of a sequence of regressions and transgressions (Frakes *et al.* 1987; Campbell & Haig 1999). The Jurassic formations are consistent with a non-marine, fluvial-lacustrine depositional environment while the Cretaceous formations are consistent with a cyclical marine environment (Senior *et al.* 1977; Krieg *et al.* 1995). Precious opal has been found within three formations (Figure 2): (1) the early Cretaceous kaolinite-rich, marine Bulldog Shale in the Eromanga Basin (Coober Pedy opal fields) where the opal layer is typically found within cracks and joints proximal to the interface between heavily weathered and partially weathered shale (Barnes & Townsend 1990; Robertson & Scott 1990), (2) the late Albian to Cenomanian volcaniclastic Winton Formation (Exon & Senior 1976) in the Eromanga Basin (Queensland opal fields) where it is typically found within the upper 1–2 m of a claystone layer underlying a sandstone layer, and (3) within the late Albian kaolinite-rich flood-plain Finch Claystone (Griman Creek Formation) in the Surat Basin (Lightning Ridge opal fields) where it typically occurs in fractures. The Mintabie opal field on the edge of the Eromanga Basin of South Australia (Figure 1) is exceptional as the opal is found within Ordovician fluviodeltatic sandstones of the Mintabie Beds (Barnes & Townsend 1990) and thus the oldest opal host rocks in central Australia. The sedimentary succession of the Eromanga and Surat basins has experienced intense weathering that has resulted in extensive silicification throughout the Tertiary regolith (Thiry *et al.* 2006) with the widespread development of silcrete caps (shin crackers) that are characteristic of the outback landscape (Senior & Mabbutt 1979). A major period of uplift between 100

Period	Age	Eromanga Basin (SW)			Eromanga Basin (NE)			Surat Basin			
Cretaceous	Cenomanian	Rolling Downs Group	Winton Formation	*Fluvial to lacustrine*	Rolling Downs Group	**Winton Formation (Opal-bearing)**	*Fluvial to lacustrine*				
	Albian		Mackundra Formation	*Marine to coastal paralic*		Mackundra Formatoin	*Marine to coastal paralic*	Rolling Downs Group	Griman Creek Formation	Coocoran Claystone	*Fluvial floodplain*
			Oodnadatta Formation	*Shallow marine*		Allaru Mudstone	*Shallow marine*			Wallangulla Sandstone	*Fluvial floodplain*
			Coorikiana Sandstone	*Shallow marine*		Toolebuc Formation	*Shallow marine*			**Finch Claystone (Opal Bearing)**	*Fluvial floodplain*
			Bulldog Shale (Opal-bearing)	*Marine*		Wallumbilla Formation: Coreena Member	*Marine to coastal paralic*			Griman Creek Fm. (Lower)	*Paralic*
	Aptian								Surat Siltstone		*Shallow marine*
	Barremnian					Wallumbilla Formation: Doncaster Member	*Shallow marine*		Wallumbilla Formation	Coreena Member	*Marine to coastal paralic*
										Doncaster Member	*Shallow marine*
	pre-Barremnian	Cadna-owie Formation		*Fluvial to shallow marine*	Cadna-owie Formation		*Fluvial to shallow marine*	Bungill Formation			*Marine transgressive*
		Algebuckina Sandstone		*Fluvial to lacustrine*	Hooray Sandstone		*Fluvial*	Mooga Sandstone			*Fluvial*

Figure 2 Summary of Cretaceous stratigraphic units and their depositional environments in the Surat Basin at Lightning Ridge, the Eromanga Basin in Queensland (NE) and the Eromanga Basin in South Australia (SW). In the South Australian part of the Eromanga Basins, the Oodnadatta, Mackundra and Winton formations have been completely eroded. Formations known to be opal-bearing are shown in bold. Adapted from Exon & Senior (1976) and Alexander & Sansome (2006).

Downloaded by [University of Sydney] at 15:42 05 September 2013

TAJE_A_754793.3d (TAJE) 02-05-2013 23:56

and 65 Ma resulted in erosion and removal of up to 3 km-thick sequence of sedimentary rock (e.g. Raza *et al.* 2009) that was eventually deposited within the Ceduna Basin (Norvick & Smith 2001). Due to its low uranium content Australian sedimentary opal has not been dated radiometrically (Gaillou *et al.* 2008a) so its age is potentially anywhere between 130 Ma to 1 kyr B.P. based on the age of the host rocks in the major opal fields (Exon & Senior 1976; Thiry *et al.* 2006), associated minerals (Newberry 2004), silcrete genesis (Senior & Mabbutt 1979; Thiry *et al.* 2006) and carbonaceous material inside cracks in opal (Dowell *et al.* 2002).

Although there has been considerable research on the geochemistry and microstructure of opal (e.g. Smallwood *et al.* 1997; Erel *et al.* 2003; Brown *et al.* 2004; Gaillou *et al.* 2008a, b) its formation in the geological environment is still poorly understood. However, its occurrence close to the surface in association with a strongly altered kaolinite-rich profile suggests that weathering is the main process driving the local supply of vast volumes of silica-rich fluids and the subsequent formation of opal (Darragh *et al.* 1966; Thiry & Milnes 1991; Gaillou *et al.* 2008a). It typically forms in regions of high porosity and permeability enhanced through localised faulting and fracturing and dissolution of unstable mineral phases in volcanogenic sedimentary rocks. Darragh *et al.* (1966) suggest that concentration of silica spheres would have been facilitated through evaporation during episodes of aridity with the formation, growth and settling of silica spheres in a confined space ultimately resulting in a prospective opal deposit.

SPATIAL DATA MINING

Background

Over the past decade, extensive high-resolution geological datasets for eastern Australia have been compiled and published. Complementing this are significant increases in computational power and the ability of computers to rapidly analyse and synthesise vast amounts of data. Geographical Information Systems (GIS) provide a platform for the simultaneous visualisation, assessment and integration of multiple datasets, having found extensive use in analysing the wide varieties of spatial datasets typically required for mineral exploration in general. Bonham-Carter (1995) outlines two primary approaches to building a predictive explorative model using GIS software: knowledge-driven models and data-driven models. The former approach is based on human expertise in assigning weightings to various associations and is generally used when the formation of the mineral deposit is well understood and constrained. The latter is based on empirical, exploratory data analysis and statistics, and an extrapolation of associations or correlations that are determined within given data sets.

The basic principle involved in both approaches is to use known or pre-determined geological associations and correlations between mineral deposits as a proxy for determining or constraining where else they are likely to have formed. Gardoll *et al.* (2000) describe the broad methodology and underlying principles used in prospectivity analysis of mineral deposits, using gold within the Yilgarn Craton in Western Australia as a case study. This concept is typically used in the economic geological community as a tool for classifying and for predicting potential prospective orogenic gold deposits. The maturity of orogenic gold deposit exploration pertains to long-term investments in exploration and data acquisition owing to the attractive commercial opportunity. This is predominantly as a consequence of the global economic significance and cultural importance that gold possesses but is also due to the wealth of data (e.g. Groves *et al.* 1998) that are available concerning the geology of orogenic gold deposits.

Groves *et al.* (2000) used stress mapping of the Yilgarn Block in Western Australia to statistically confirm associations between structural features and orogenic gold deposits. The prospectivity map that was developed as a result of these associations classified 80% of produced gold from the Yilgarn Block into the zone of highest prospectivity (Groves *et al.* 2000). Similarly, Bierlein *et al.* (2006) used fault zone and gravity gradient data, to determine that a preferential distribution for orogenic gold in the Yilgarn Block occurs in small faults that are influenced by longer, more deeply penetrating faults in their proximity. In an alternative approach, Holden *et al.* (2008) used only regional aeromagnetic data over the same area to identify zones of high prospectivity based on the degree of magnetic complexity in close proximity to magnetic discontinuities representing large shear zones. Their study identified the location of 76% known orogenic gold deposits based on the single aeromagnetic dataset.

Outside Australia, there have been similar studies focussing on associations between Carlin-type gold deposits and deep-seated crustal structures in North America (Crafford & Grauch 2002), as well as between shear zones and gold deposits in Canadian Archean greenstone belts (Harris *et al.* 2001). A fuzzy logic approach has been used to combine incomplete or uncertain datasets in order to constrain and develop prospectivity maps for gold deposits based on proximity to geological features in the Philippines (Carranza & Hale 2001) and in prospectivity modelling for iron-oxide copper gold (IOCG) deposits in Finland (Nykänen *et al.* 2008). The approach taken by Nykänen *et al.* (2008) is similar to this study, in that various data layers are prepared separately and then amalgamated together using GIS software to highlight areas of high and low prospectivity. An important difference, however, between Australian opal and the more thoroughly analysed gold deposits, is that Australian opal is associated with surficial sedimentary processes, specifically weathering, rather than deeper, large-scale mesothermal fluid movement (Groves *et al.* 1998). Consequently, there is greater dependence on small (1–10 m) microfaults, surficial geology of the study area and the development and preservation of the regolith associated with the opal-bearing Cretaceous sedimentary rocks.

Downloaded by [University of Sydney] at 15:42 05 September 2013

TAJE_A_754793.3d (TAJE) 02-05-2013 23:56

Application to opal exploration

In this study, we adapt the basic methodologies and principles described above to evaluating the prospectivity of opal within the Great Artesian Basin. Our method involves a hybrid approach in which known information about the nature of the opal host sequences is used to steer and optimise the selection of spatial datasets and relationships of interest, but also involving the extraction of several proxy-features from spatial and spatio-temporal datasets that demonstrate significant associations. In this way, a limited conceptual understanding is complemented by a data-mining approach, with the potential to develop a predictive targeting model and to expose associations that may ultimately lead to better overall understanding of the underlying physical processes. This is the first systematic attempt at linking multi-layered data to known distributions of opal, thus providing a map of potential areas for future opal mining. Several informal attempts have been made to associate opal occurrence with particular features such as mesas and localised fracture networks for small-scale exploration. D. Horton (pers. comm. 2011) identified large (~100 km) topographic domes present at most of the major opal localities (e.g., Lightning Ridge, Quilpie, Winton) and suggested that further exploration could focus on identifying other domes throughout the Great Artesian Basin as prospective locations for opal. Smaller scale opal exploration (of the order of 10 km) has previously been approached in many different ways. Pecover (1996) outlined a scenario of opal formation based on fluid concentrations and pressure gradients through fissures and microfaults, suggesting that opal exploration should focus on areas of the Great Artesian Basin that have experienced high degrees of stress and that exhibit significant brecciation. Similarly, J. J. Watkins (pers. comm. 2011) suggested that opal exploration should focus predominantly on identifying structural lineaments as targets for potential opal deposits. D. Robson (pers. comm. 2011) proposed that exploration efforts (of the order of 1 km) could use local, airborne, high resolution magnetic surveying to determine the location of faults existing within the upper ~30 m of the weathered profile. This is similar to the models proposed by J. J. Watkins (pers. comm. 2011) and Pecover (1996), in that the fluid movement along faults is treated as a primary criterion in opal formation, and therefore a useful tool in opal exploration. Finally, Senior & Chadderton (2007) outline how gamma ray logging of drill holes can be used for precise opal exploration (on a 1 m scale) by locating the contact between a sandstone and claystone layer where opal is typically found (Senior *et al.* 1977; Barnes & Townsend 1990).

The approach that is being used here is to provide a 'greenfield' exploration methodology for opal exploration to assist in finding new potential opal localities in an efficient fashion over a large area. Importantly, the methodology proposed here is flexible in that it allows different combinations of base map layers to be integrated. This is an important feature for such a new study based on data of relatively low resolution.

Methodology

Our prospectivity mapping approach is based on establishing associations between particular features in individual map data layers with known opal mining sites. We assume that different layers represent independent data sets, thus allowing a succession of these layers to be combined in order to reduce an overall integrated layer comprising a combination of the base layers. The final layer is produced via a weighted sum of base layers, allowing a degree of confidence/uncertainty to be encoded. The datasets used in creating the layers each have their own accuracies and shortcomings, and have in some cases involved interpretations and extrapolations leading to a non-uniform spatial accuracy. Thus, the layer combining method proposed in this paper takes a flexible approach where data layers can be added/removed/weighted at ease during the experimentation phase.

In this study, a training set comprising all known opal localities (1036 opal mines) was assembled using published maps from state geological surveys (Carr 1979; Robertson & Scott 1989; Carter 2005; Geological Survey of Queensland 2012). The location of each opal mine was digitised and geo-referenced using GIS software. Opal mines from Mintabie, Lambina and the smaller opal mining districts in the vicinity of Stuart Creek and White Cliffs were omitted as their locations were missing from published maps and reports. A necessary assumption made for the data-derived generation of prospectivity maps is that this dataset represents an unbiased and representative sample of an underlying population. There are, however, some limitations. Australian state laws limit extensive opal mining in many locations. For example, opal mines around Lighting Ridge tend to have a large cluster of individual mines within a relatively small area. However, the potential sample bias resulting from this local clustering of mines is alleviated by the large set of spatially well-separated mine site clusters across the Great Artesian Basin, sampling a wide range of formations (Figure 3).

Data layers

Six data layers have been used in the opal data mining analysis: regional geology (Figure 3a), soil type (Figure 4a) regolith type (Figure 4b), topography (Figure 5a), radiometric data (Figure 5b) and paleogeography (Figures 6, 7a). Faults were not included because there is no dataset available at the small scale associated with opal deposits. Each layer has been clipped to a bounding box [(131.5106°E, 17.8604°S), (151.8217°E, 32.6709°S)] that encompasses the extent of Cretaceous sedimentary rock (the predominant chronostratigraphic opal host; Figure 2) within the Eromanga and Surat basins, thus minimising computational time. The base layer of the prospectivity map is a 1:1 000 000 digital geological map of Eastern Australia (Figure 3a). Each subsequent layer was then added on top of this layer in order to minimise the targeting area (Table 1). For each layer the probability of opal occurrence was determined using the associations and

Downloaded by [University of Sydney] at 15:42 05 September 2013

TAJE_A_754793.3d (TAJE) 02-05-2013 23:56

attributed a probability value between 0 and 1. For the purpose of brevity, the combination of Surat and Eromanga basins will be referred to as the Great Artesian Basin. However, it should be noted that the Great Artesian Basin also includes the Carpentaria Basin to the north, which is not known to contain opal.

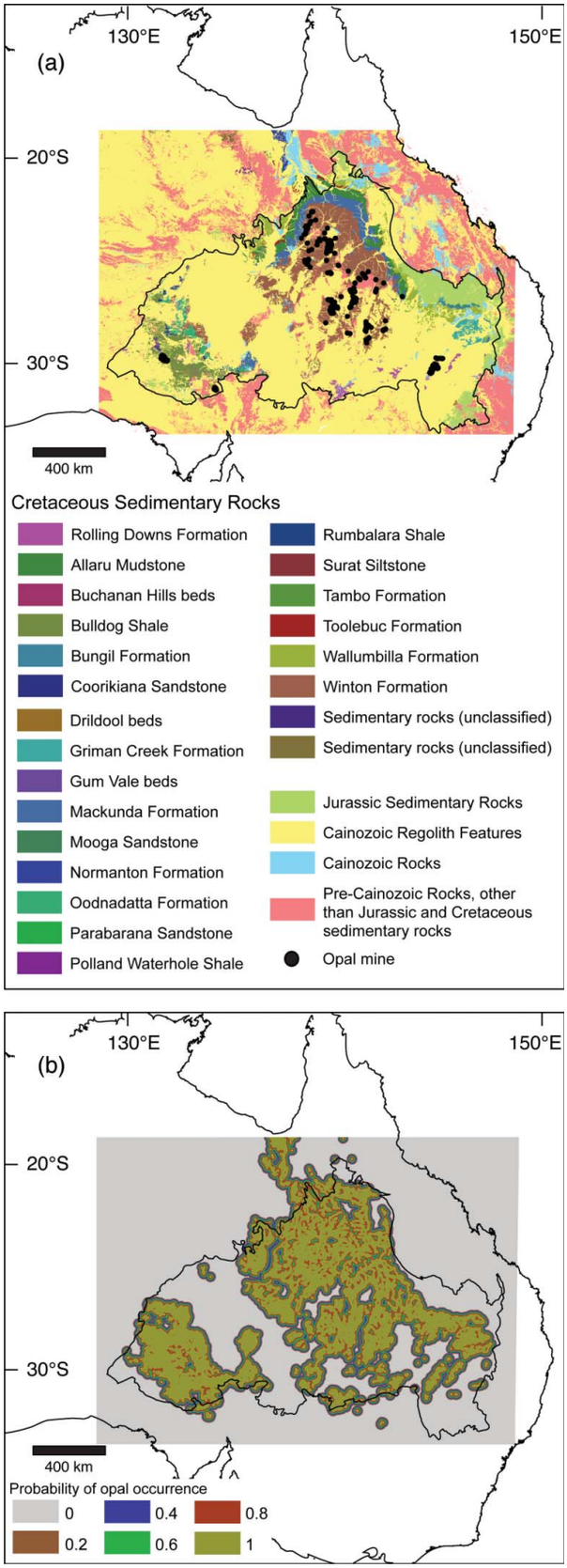

LAYER 1: GEOLOGY OF EASTERN AUSTRALIA

The digital 1:1 000 000 geological map of Australia (Raymond & Retter 2010) used for this study was acquired from Geoscience Australia. The dataset covers the geological units throughout the entire continent, and the metadata include relative and absolute ages of most formations, a brief lithological description and the sub-group, group name and super-group (where appropriate) of the formations. This dataset was created by the amalgamation of the pre-existing 1:250 000 geological maps of Australia. In generating the layer used for the prospectivity map, the geological map was clipped to the bounding box. The Cretaceous sedimentary rock formations that have a minimum age ranging from the Albian to Cenomanian were attributed a probability value of 1. All formations/units older than Cretaceous were given a probability value of 0. Areas characterised by patches of thin Cenozoic cover were assigned probabilities between 0.8 and 0.2 depending on their distance from the nearest Cretaceous surface outcrop (Figure 3).

LAYERS 2 AND 3: REGOLITH AND SOIL TYPES

The regolith dataset used in the analyses is the digital compilation of the Regolith Site Classification Map (Kilgour & Pain 2000). The dataset contains a qualitative classification of the Australian landscape based on differing regolith features such as major and minor landforms, soil types and a description of the regolith. Two data layers were created based on qualitative associations between opal and the regolith type/soil classification. The first layer is based on a description of the regolith and the second is a classification of the soil (Figure 4). Using the data-mining suite (Landgrebe & Müller 2011) incorporated as part of the GPlates PaleoGIS software (Boyden *et al.* 2011), six regolith features and nine types of soil (see Figure 4) were determined to be associated with the presence of opal, and all were subsequently attributed probability values of 1. Note that our original opal dataset excluded two additional regolith classifications that are associated with precious opal as described by Kilgour & Pain (2000) but for which we do not have exact locations of opal mines (White Cliffs). These two areas were attributed probability values of 0.5. All other classifications of both regolith and soil were given probability values of 0 (Figure 4c, d).

Figure 3 Association between opal occurrences and regional geology within the Great Artesian Basin. Note the black outline of combined Eromanga and Surat basins. (a) Known locations of opal mines superimposed over major sedimentary Cretaceous units. Geological data from Raymond & Retter (2010). (b) Probability of opal occurrence (from 0 to 1) in relation to regional geology. The grey rectangle defines the bounding box that was use to clip the continent-wide data set. Because the opal is strongly associated with Cretaceous sedimentary rocks, a very large area of opal prospectivity is identified.

Downloaded by [University of Sydney] at 15:42 05 September 2013

TAJE_A_754793.3d (TAJE) 02-05-2013 23:56

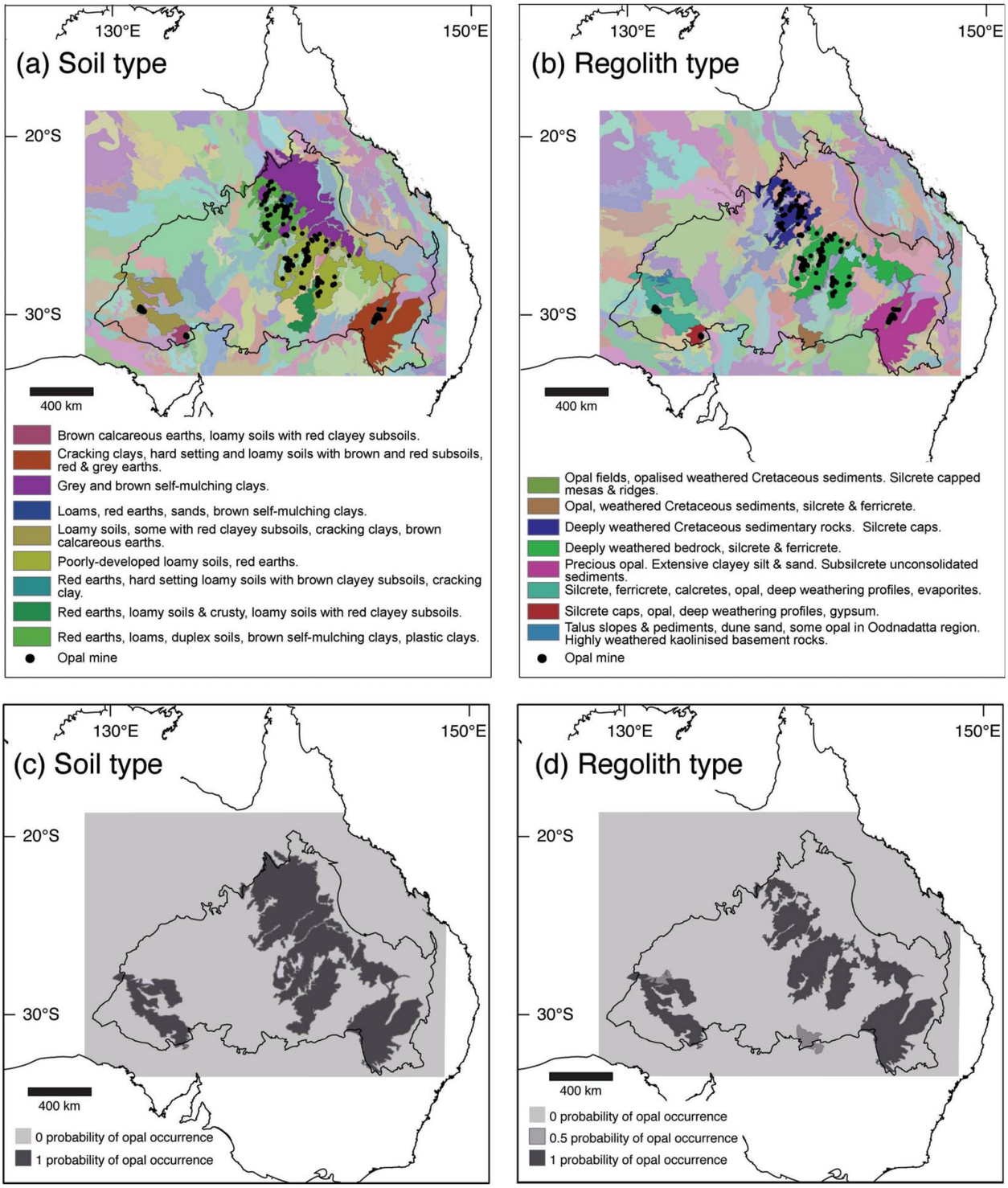

Figure 4 Association between opal occurrences and soil type and regolith type within the Great Artesian Basin. Note the black outline of combined Eromanga and Surat basins. (a) Known locations of opal mines superimposed over soil types, predominantly loamy soils and red earths. (b) Known locations of opal mines superimposed over regolith type. Opal shows a strong association with weathered Cretaceous profiles, silcrete and ferricrete. (c) Probability of opal occurrence (from 0 or 1) in relation to soil type. The grey rectangle defines the bounding box that was use to clip the continent-wide data set with high-probability areas centred around 9 soils types. (d) Probability of opal occurrence in relation to regolith type. Soil and regolith data sets from Kilgour & Pain (2000).

An additional quantitative layer developed for this dataset is based on proximity of opal to a regolith boundary. This association was determined through data mining of the opal locations relative to a change in regolith type, which indicates that the average distance from any opal location to a regolith boundary is 11 km, with a standard deviation of 7 km. To reflect this association, an internal multiple ring buffer of five

Downloaded by [University of Sydney] at 15:42 05 September 2013

TAJE_A_754793.3d (TAJE) 02-05-2013 23:56

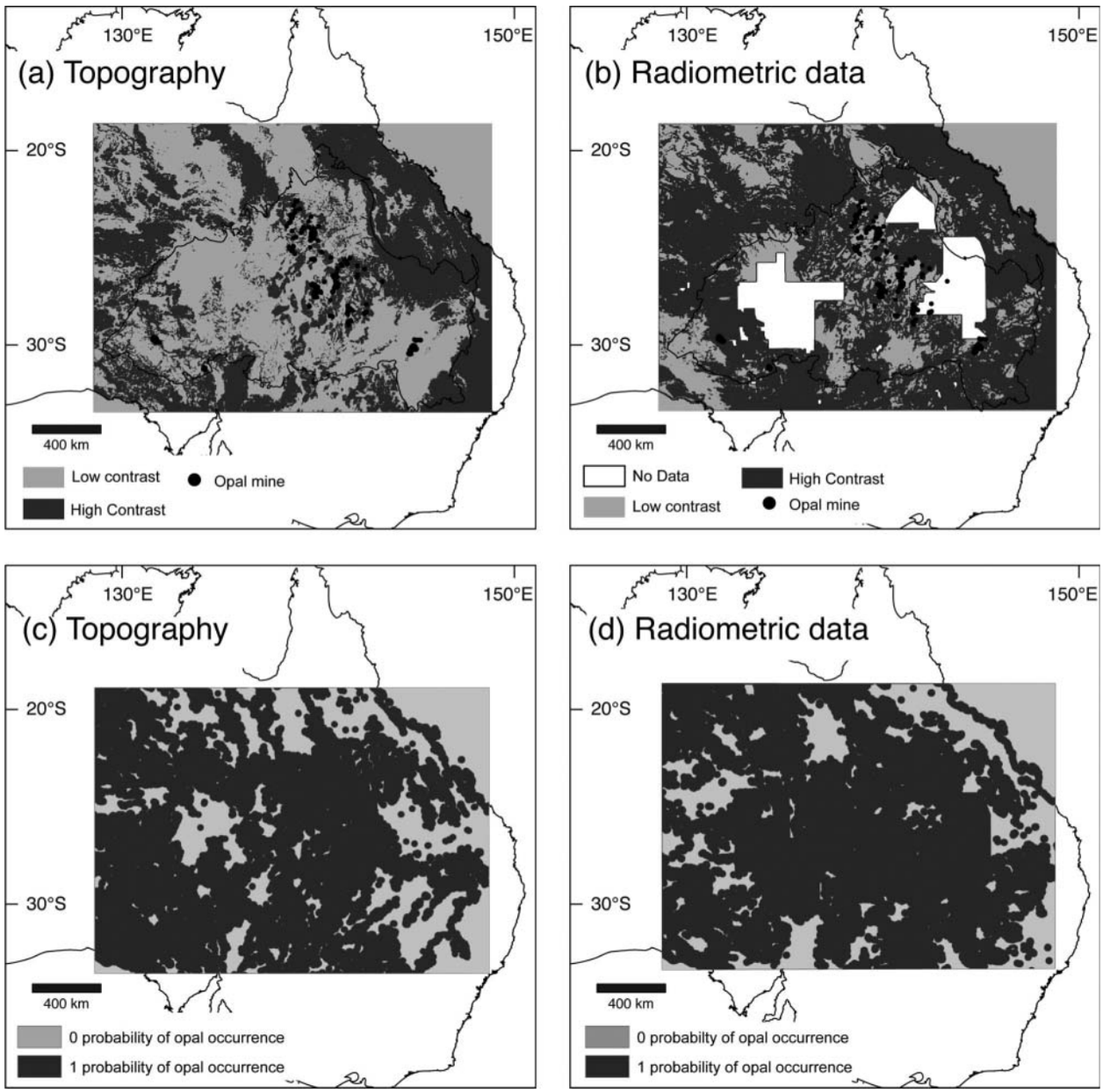

Figure 5 Association between opal occurrences and topography with a resolution of 250 m (a) and radiometric data with a resolution of 80 m (b) within the Great Artesian Basin. Probability of opal occurrence in relation to topography (c) and radiometric data (d). Topography data set from Hutchinson *et al.* (2006); radiometric data set from Minty et al. (2010).

increments up to a maximum distance of the computed mean added to two standard deviations ($\mu + 2\sigma$) was computed, resulting in the generation of 0.05° (roughly 5 km) buffers. The zones closest to a regolith boundary were attributed a probability value of 1 with the probability assigned to the 5 km wide buffer regions progressively decreasing in increments of 0.2 away from a given regolith boundary.

LAYERS 4 AND 5: GEOPHYSICAL DATASETS

The topography dataset used in the analysis has a resolution of 250 m (Hutchinson *et al.* 2006), while the radiometric dataset, representing a levelled and merged composite grid of the potassium component, has a resolution of 80 m with three large areas without data (Minty 2011) mostly affecting our analysis of the opal regions in the vicinity of Quilpie in southern Queensland (Figure 5). The potassium radiometric component was selected for this analysis after investigating the correlation of local gradients in potassium, uranium and thorium radiometric grids with opal deposits, which revealed the strongest correlation with the potassium data set. For both the topography and radiometric datasets we calculated the contrast ratio for each pixel by taking an 8 km square around each pixel and dividing the 80th percentile pixel by the 20th percentile pixel. The resulting map was binarised using a 50% threshold to

Downloaded by [University of Sydney] at 15:42 05 September 2013

TAJE_A_754793.3d (TAJE) 02-05-2013 23:57

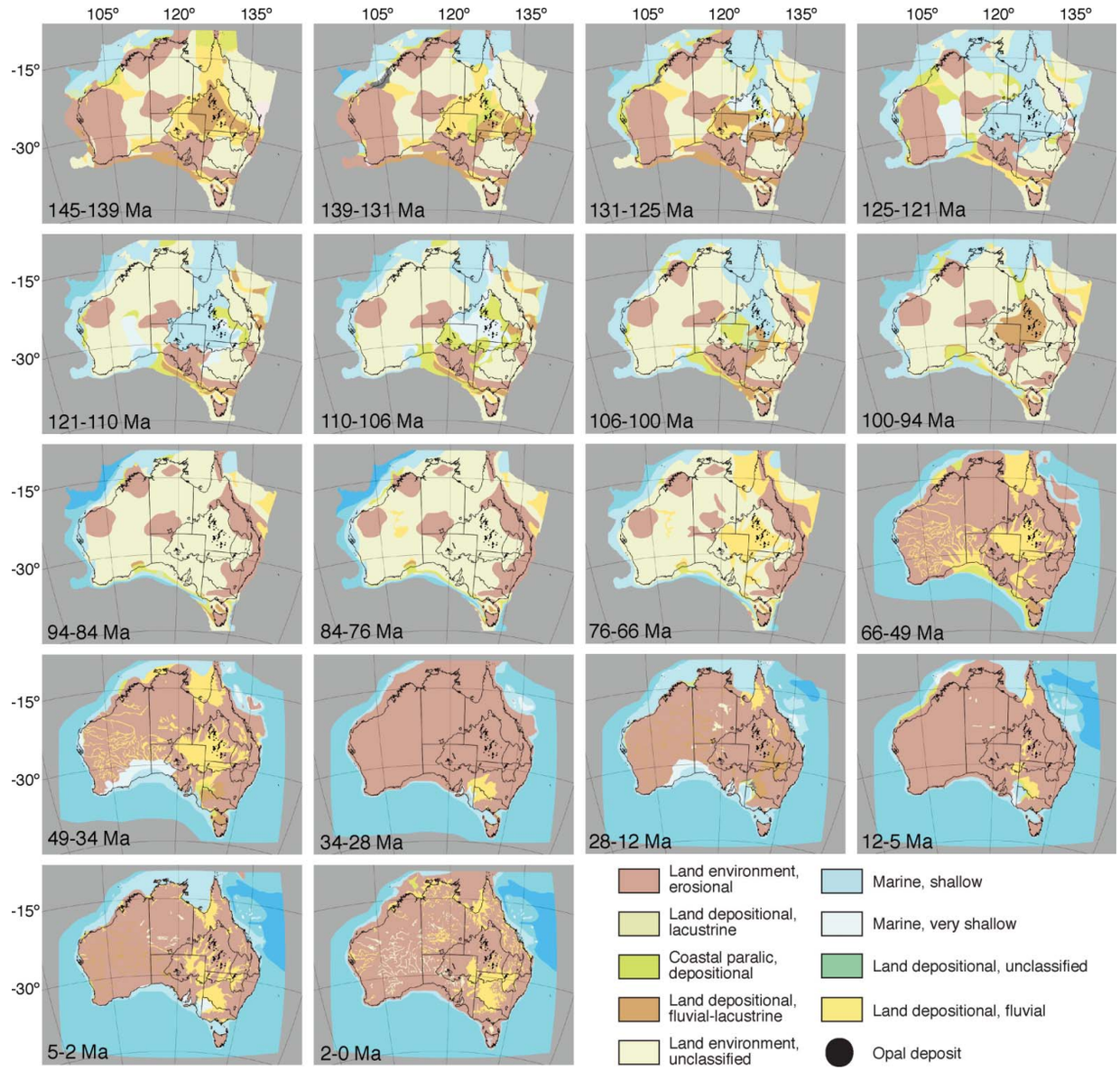

Figure 6 Depositional and erosional environments from 145 Ma to the present day showing flooding of Eromanga and Surat basins (thin black outline within the Australian continent with black dots representing opal mine localities) from about 131 Ma to 100 Ma followed by progressive uplift and extensive erosion linked to the cessation of subduction east of Australia (Matthews *et al.* 2011) until the present day. Depositional environments within the opal mining regions have been dominated by marine and fluvial processes. Adapted from Langford et al. (1996). Note that 18 out of a total of 19 time slices are shown here.

outline areas of the Great Artesian Basin with high and low contrast ratios. The association suggests that opal occurs at locations where there is a gradient change, from a high to low contrast ratio. We used the mean plus one standard deviation (which in total is 18 km) of the computed distance from an opal location to a regolith boundary to create a buffer zone around the boundaries of the high- and low-contrast areas. Areas within the buffer zones were attributed probability values of 1, and areas outside the buffer zones were attributed values of 0 (Figure 5).

LAYER 6: PALEOGEOGRAPHY

The paleogeography dataset (Langford *et al.* 1996) is a digital version of a compilation of maps based on reconstructions of the depositional/erosional environment, of the Australian continent through time from 542 Ma to present day, comprising 70 time slices. As opal is found predominantly in Cretaceous sedimentary rocks, the analysis of the dataset and generation of the data layer was constrained from 145 Ma to the present day, comprising 19 time slices that include shallow marine, coastal,

Downloaded by [University of Sydney] at 15:42 05 September 2013

TAJE_A_754793.3d (TAJE) 02-05-2013 23:57

Table 1 Effect of various input layers on the area of opal prospectivity for the Great Artesian Basin.

Data layer	Area of the Great Artesian Basin (km^2) $\times 10^4$
Great Artesian Basin	135.5 (100%)
Geology buffer	104.1 (76.8%)
Regolith soil	49.5 (36.5%)
Regolith type	35.4 (26.1%)
Palaeogeography	14.5 (10.7%)
Radiometric data	126.5 (93.4%)
Topography	106.6 (78.7%)
Prospectivity[a]	8.1 (6%)

[a] All data sets (layers) combined.
In the initial analysis, the entire Great Artesian Basin is considered to be prospective for opal exploration. This area is reduced to 6% with the combination of all data sets.

Downloaded by [University of Sydney] at 15:42 05 September 2013

lacustrine and fluvial depositional environments and a period of intense erosion from at least 65 Ma until the present day (Figure 6). A concept related to the formation of opal is that only a particular sequence of depositional/erosional environments will lead to conditions suitable for opal formation. We test this idea by extracting paleogeographic time sequences from the paleogeographic dataset at each opal locality. These time series consist of the time-varying geographic environment properties extracted from the paleogeographic time-slices. This first step resulted in a total of 1036 time-series, one for each opal mine with 19 time slices spanning the period of interest (Figure 6). In this analysis, we are concerned with the transition of environments, rather than the duration of each period, following the assumption that it is the sequence of transitions that ultimately create geological conditions favourable for opal formation. Therefore, we map the depositional environment time series to 'ordinal' event sequences, consisting of ordered lists of events in chronological order (Figure 7).

RESULTS

The combination of the six data layers effectively reduces the baseline targeting area (the Great Artesian Basin) to a mere 6% (8×10^4 km^2) representing the final opal prospectivity map (Table 1; Figure 8). The greatest reduction of 89% in the target area is achieved with the paleogeography data set, thus highlighting the importance of the depositional/erosional sequence on the formation and preservation of opal (Figure 7). Amalgamating the various ordinal event sequences (Figure 7) illustrates that there is considerable similarity between paleogeographic sequences across all opal localities. Of the 1036 opal mine localities, 52 independent ordinal sequences are identified, and of these, 27 sequences describe 95% of all independent ordinal paleogeographic sequences. It follows that these 27 sequences (Figure 7) comprising fluvial and shallow marine depositional sequences followed by a prolonged phase of erosion are representative of the depositional/erosional sequences underpinning for opal formation. The prospectivity map does not predict the location of opal at White Cliffs (Figure 8).

The White Cliffs opal mining region is absent from our set of known locations of opal mines, as its exact location has not been recorded on published maps, but it is represented by a large patch on the regolith type map of Kilgour & Pain (2000) (Figure 4b). The White Cliffs paleogeographic sequence has alternated between an erosional and fluvial environment three times since the regression of the inland sea *ca* 90 Ma (Figure 6), while other opal mining regions experienced only one marine–fluvial–erosional transition (Figure 6). In addition, although there are similarities between the soil in the White Cliffs area and in other locations, such as the presence of red earths and red clayey subsoils (Figure 4a), its absence from the classification based on the soil type data layer arises from it being primarily associated with crusty, loamy soils. The White Cliffs region is located near the southern edge of the Great Artesian Basin (Figure 1) and, being one of the most proximal areas to the paleo-coastline, would have experienced more complex and more frequent shifts in depositional environments. As a consequence, the paleogeographic transitions and hence the soil types are different from the other opal mine locations that are used to train our classification algorithm.

The paleogeographic sequences assist greatly in minimising the exploration area, highlighting areas of higher prospectivity, owing to the similarity of paleogeographic histories between most areas where opal has already been found. However, there are areas in the Great Artesian Basin that may contain opal whose prospectivity clearly cannot be determined using paleogeographic sequences alone.

The regolith type layer is the next most effective layer at reducing the targeting area (74%; Table 1) followed by the soil type layer (64%; Table 1). The large area reduction achieved using the regolith/soil dataset may be due to the detailed regolith type and soil-type classifications available for the Great Artesian Basin resulting in a relatively high degree of specificity for the opal-bearing regions. More importantly, however, it confirms that opal occurrence is strongly associated with weathering history and the parent rock type, which together are critical in supplying vast amounts of silica required for the formation opal deposits. Each opal field is characterised by a single regolith feature (Figure 4). In general, regions of high opal prospectivity are associated with red earth and loamy soils and deeply weathered profiles that frequently contain ferricrete and silcrete horizons (Figure 4).

The lowest area reduction of 7% (i.e., 93% of the target area remains prospective) is achieved with the radiometric dataset (Table 1), which contains large areas without data (Figure 5), although in general opal deposits appear to be associated with geochemical gradients, reflected by variations in radiometric data that mimic topographic gradients (Figure 5) and regolith type changes (Figure 4). Typically, the change in regolith is from deeply weathered sedimentary rock within which opal is found, to unconsolidated colluvium and alluvium, and aeolian sand or silicified Paleogene/Neogene sedimentary rocks. Likewise, the geological layer reduced the area of

TAJE_A_754793.3d (TAJE) 02-05-2013 23:57

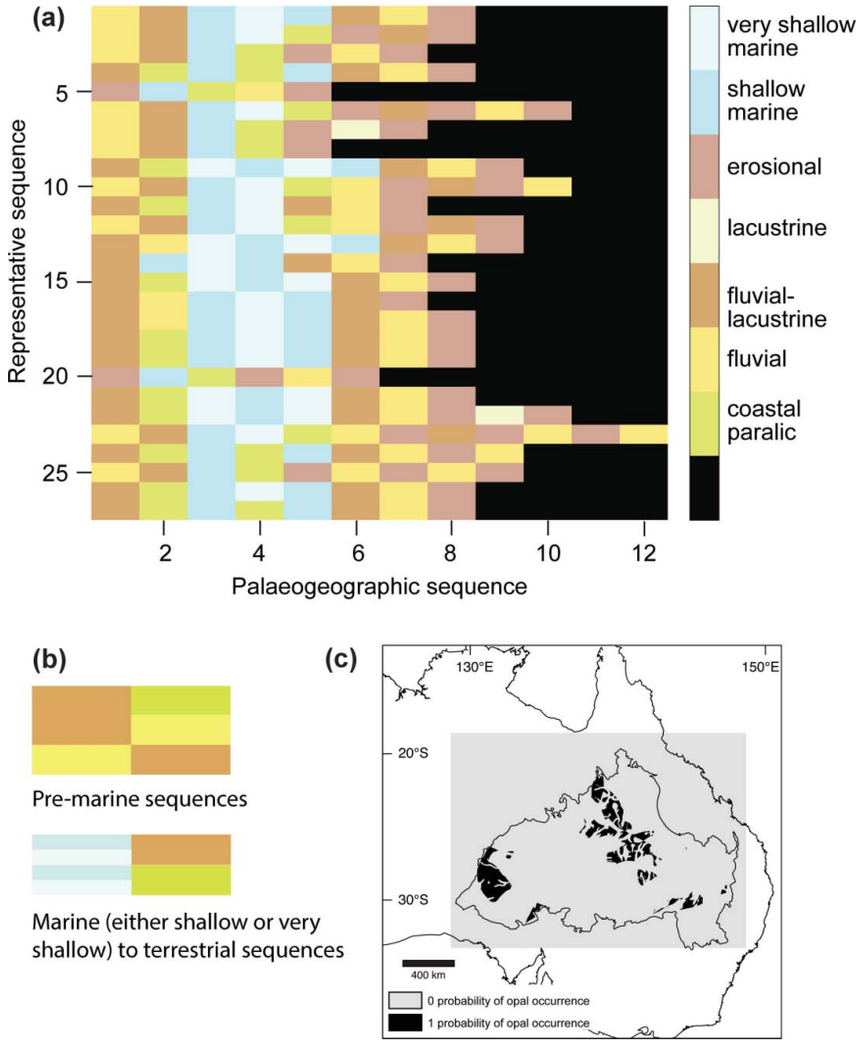

Figure 7 Association between opal occurrences and particular sequences of depositional/erosion events through time. (a) Graphical representation of the 27 chronological paleogeographic sequences that represent 95% of opal localities based on the maps of depositional environments shown in Figure 6. Each row depicts a sequence of depositional environments (colour-coded and corresponding to the scheme used in Figure 6), with columns representing their superposition through time at any given opal mine locality. The sequences show that the overall paleogeographic evolution can be characterised by an initial fluvial/lacustrine environment, followed by a marine inundation with a subsequent return to fluvial/lacustrine conditions followed by a regression leading to an erosional environment. These ordinal sequences disregard the duration of each depositional/erosional period, and instead reflect the sequence of events that marks the change from one sedimentary/erosional regime to another. All sequences start at 145 Ma and end at 0 Ma. The fewer events have occurred at a given locality the shorter the total sequence of events is (i.e., total length of horizontal coloured bars). (b) Representative set of environments (legend as for Figure 7a) associated with known opal occurrences. Pre-marine sequences refer to terrestrial sequences that pre-date the main transgression phase in the Great Artesian Basin. Marine to terrestrial sequences refer to the main transgressive phase and subsequent regression, respectively. For the pre-marine transition, 24 out of the 27 unique temporal signatures of the opal localities are characterised by three transitions: fluvial to fluvial-lacustrine (10 out of 27 signatures), fluvial-lacustrine to coastal-paralic (11 out of 27 signatures), and fluvial-lacustrine to fluvial (3 out of 27 signatures). For the marine to terrestrial transitions, the opal localities are characterised by only two different transitions: marine to fluvial-lacustrine (13 out of 27 signatures), and marine to coastal-paralic (14 out of 27 signatures). In contrast, areas not associated with known opal occurrence are characterised by large variability in environmental transitions. (c) Probability of opal occurrence based on the 27 chronological paleogeographic sequences that represent 95% of opal localities *vs* paleogeographic sequences that are associated with non-opal-bearing region.

prospectivity by a relatively moderate amount (23%, Table 1).

Interestingly, the combination of the geology, regolith and soil layers only minimally reduces the targeting area. This indicates that opal formation as a consequence of weathering could have occurred throughout nearly the entire extent of Cretaceous sedimentary rock in the Great Artesian Basin. The addition of the paleogeographic data significantly reduces the total prospective area (Table 1), indicating the importance of specific sequences of sedimentary/erosional environments in giving rise to regolith conditions conducive to opal formation.

Downloaded by [University of Sydney] at 15:42 05 September 2013

TAJE_A_754793.3d (TAJE) 02-05-2013 23:57

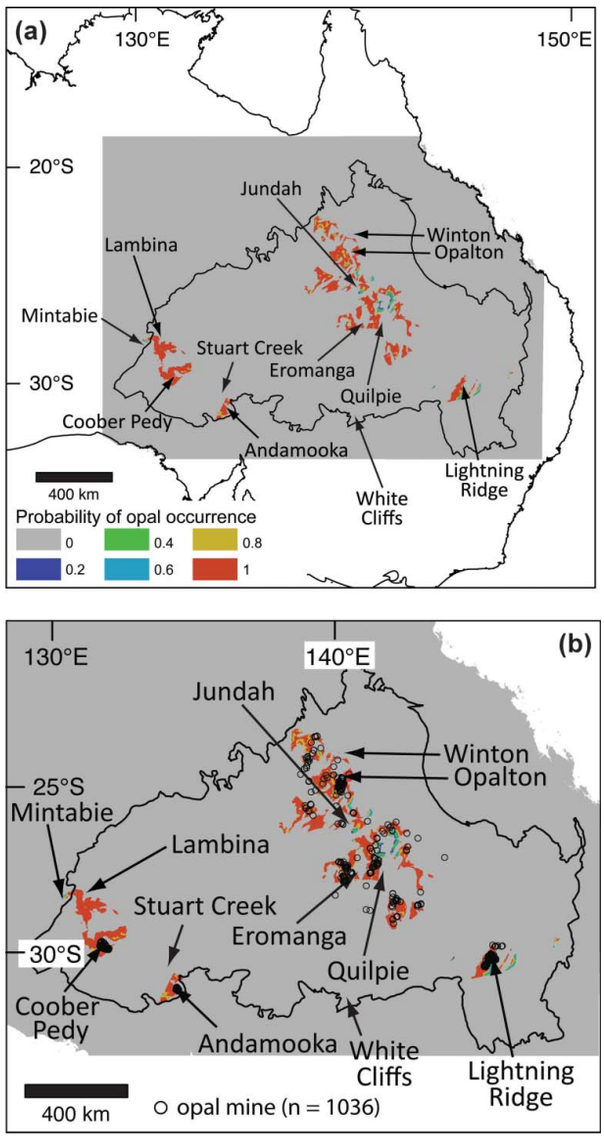

Figure 8 (a) Opal prospectivity map based on assimilation of geological, soil type, regolith type, topographic, radiometric and paleographic datasets. For clarity, opal mine locations have been omitted. (b) Same map as in (a) also showing known locations of opal mines. The major mining centres around Lambina and Mintabie have been correctly identified. They were omitted from the input dataset as the accurate location of opal mines was not known from existing maps and reports. A large region northeast of Coober Pedy appears to be highly prospective as do several large areas proximal to known opal fields within the eastern part of the Eromanga Basin in Queensland.

In the southwestern Eromanga Basin in South Australia, the prospectivity map correctly predicts the location of opal occurring at both Lambina and Mintabie (Figure 8). In addition, the map indicates a northwest–southeast-oriented corridor stretching from Coober Pedy to the Mintabie/Lambina area that is highly prospective for opal. Similarly, there is a northwest–southeast-oriented corridor of prospectivity from the Winton/Opalton area extending towards Quilpie (Figure 8). Geologically, the Lightning Ridge opal mining region is distinct from the surrounding plains of Quaternary colluvium material (Burton 2011), resulting in a very small area of potential prospectivity for opal.

CONCLUSIONS

We have generated an opal prospectivity map through the combination of large digital geological and geophysical data sets, including space–time sequences of depositional environments, with a novel data mining workflow. The weighted combination of all data layers reduces the total area prospective for opal to 6% of the Eromanga and Surat basins combined. The highest degree of opal prospectivity, and the most likely location for new opal fields, occurs along the southwestern extent of the Great Artesian Basin in South Australia, specifically between the Coober Pedy and Lambina and Mintabie fields. The maps also suggest that further exploration for opal may be prospective in a northwest–southeast corridor throughout central Queensland. Our data-layering methodology is flexible and allows for the generation of multiple prospectivity maps through the compilation of different data layers, determined by personal interpretation of the strength of each association. To date, opal exploration has been entirely focused on the local scale of the deposits based on local features such as faulting, topography, shallow stratigraphy or proximity to known opal deposits. Our approach places opal exploration in a spatio-temporal context by considering basin evolution and basin-wide geological and geophysical datasets. Although still rudimentary, our methodology has the potential to diversify current approaches towards opal exploration, identifying new greenfield targets and, hence, optimising subsequent, higher cost, detailed investigations.

ACKNOWLEDGEMENTS

We would like to thank opal miners and opal miners associations in Coober Pedy, Lightning Ridge and Winton for their generosity in sharing information and for showing us around key opal mines. We are especially grateful to Colin Duff and Maxine O'Brien. We would also like to thank Anya Reading and Jon Claoué-Long for their constructive and thorough reviews, which have improved the paper significantly. This project was funded by the Australian Research Council (ARC) Discovery Grant DP0987604.

REFERENCES

Alexander E. M. & Sansome A. (Editors) 2006. *Lithostratigraphy and environments of deposition (Eromanga Basin)*. (Petroleum Geology of South Australia, Vol. **4**). Department of Primary Industries and Resources, South Australia.

Barnes L. C. & Townsend I. J. (Editors) 1990. *Opal deposits in Australia*. (Geology of the Mineral Deposits of Australia and Papua New Guinea., Vol. **1**). The Australian Institute of Mining and Metallurgy, Victoria.

Bierlein F. P., Murphy F. C., Weinberg R. F. & Lees T. 2006. Distribution of orogenic gold deposits in relation to fault zones

Downloaded by [University of Sydney] at 15:42 05 September 2013

TAJE_A_754793.3d (TAJE) 02-05-2013 23:57

and gravity gradients: targeting tools applied to the Eastern Goldfields, Yilgarn Craton, Western Australia. *Mineralium Deposita* **41**, 107–126.

Bonham-Carter G. F. 1995. *Geographic information systems for geoscientists: modelling with GIS. Computer Methods in the Geosciences Volume 13*. Pergamon, New York.

Boyden J. A., Müller R. D., Gurnis M., Torsvik T. H., Clark J. A., Turner M., Ivey-Law H., Watson R. J. & Cannon J. S. 2011. Next-generation plate-tectonic reconstructions using GPlates. In: Keller G. R. & Baru C. eds., *Geoinformatics: Cyberinfrastructure for the Solid Earth Sciences*, pp. 95–114. Cambridge University Press, Cambridge.

Brown L. D., Ray A. S. & Thomas P. S. 2004. Elemental analysis of Australian amorphous banded opals by laser-ablation ICP-MS. *Neues Jahrbuch für Mineralogie—Monatshefte* **2004**, 411–424.

Burton G. R. 2011. *Explanatory notes. Angledool 1:250 000 geological sheet SH/55-7* (2nd edition). Geological Survey of New South Wales, Maitland, NSW.

Campbell R. J. & Haig D. W. 1999. Bathymetric change during Early Cretaceous intracratonic marine transgression across the northeastern Eromanga Basin, Australia. *Cretaceous Research* **20**, 403–446.

Carr S. G. 1979. *Andamooka precious stone fields [map]*. Geological Survery of South Australia, Adelaide.

Carranza E. J. M. & Hale M. 2001. Geologically constrained fuzzy mapping of gold mineralization potential, Baguio district, Philippines. *Natural Resources Research* **10**, 125–136.

Carter P. 2005. *Opal Fields—Lightning Ridge region [map]*. Geological Survey of New South Wales, Maitland.

Crafford A. E. J. & Grauch V. J. S. 2002. Geologic and geophysical evidence for the influence of deep crustal structures on Paleozoic tectonics and the alignment of world-class gold deposits, north-central Nevada, USA. *Ore Geology Reviews* **21**, 157–184.

Darragh P. J., Gaskin A. J., Terrell B. C. & Sanders J. V. 1966. Origin of precious opal. *Nature* **209**, 13–16.

Dowell K., Mavrogenes J., McPhail D. C. & Watkins J. 2002. Origin and timing of formation of precious black opal nobbies at Lightning Ridge. Regolith and Landscapes in Eastern Australia (unpubl.).

Erel E., Aubriet F., Finqueneisel G. & Muller J. F. 2003. Capabilities of laser ablation mass spectrometry in the differentiation of natural and artificial opal gemstones. *Analytical Chemistry* **75**, 6422–6429.

Exon N. F. & Senior B. R. 1976. The Cretaceous of the Eromanga and Surat Basins. *BMR Journal of Australian Geology and Geophysics* **1**, 33–50.

Frakes L. A., Burger D., Apthorpe M., Wiseman J., Dettmann M., Alley N., Flint R., Gravestock D., Ludbrook N. & Backhouse J. 1987. Australian Cretaceous shorelines, stage by stage. *Palaeogeography, Palaeoclimatology, Palaeoecology* **59**, 31–48.

Gaillou E., Delaunay A., Rondeau B., Bouhnik-le-Coz M., Fritsch E., Cornen G. & Monnier C. 2008a. The geochemistry of gem opals as evidence of their origin. *Ore Geology Reviews* **34**, 113–126.

Gaillou E., Fritsch E., Aguilar-Reyes B., Rondeau B., Post J., Barreau A. & Ostroumov M. 2008b. Common gem opal: An investigation of micro-to nano-structure. *American Mineralogist* **93**, 1865.

Gardoll S. J., Groves D. I., Knox-Robinson C. M., Yun G. Y. & Elliott N. 2000. Developing the tools for geological shape analysis, with regional- to local-scale examples from the Kalgoorlie Terrane of Western Australia. *Australian Journal of Earth Sciences* **47**, 943–953.

Geological Survey of Queensland 2012. *Interactive resource and tenure maps [digital dataset]*. Department of Mines and Energy, Queensland.

Groves D. I., Goldfarb R. J., Gebre-Mariam M., Hagemann S. G. & Robert F. 1998. Orogenic gold deposits: A proposed classification in the context of their crustal distribution and relationship to other gold deposit types. *Ore Geology Reviews* **13**, 7–27.

Groves D. I., Goldfarb R. J., Knox-Robinson C. M., Ojala J., Gardoll S., Yun G. Y. & Holyland P. 2000. Late-kinematic timing of orogenic gold deposits and significance for computer-based exploration techniques with emphasis on the Yilgarn Block, Western Australia. *Ore Geology Reviews* **17**, 1–38.

Harris J. R., Wilkinson L., Heather K., Fumerton S., Bernier M. A., Ayer J. & Dahn R. 2001. Application of GIS processing techniques for producing mineral prospectivity maps—a case study: mesothermal Au in the Swayze Greenstone Belt, Ontario, Canada. *Natural Resources Research* **10**, 91–124.

Holden E-J., Dentith M. & Kovesi P. 2008. Towards the automated analysis of regional aeromagnetic aata to identify regions prospective for gold deposits. *Computers and Geosciences* **34**, 1505–1513.

Hutchinson M. F., Stein J. A. & Stein J. L. 2006. *GEODATA 9 second digital elevation model (DEM-9S) version 3*. Geoscience Australia, Canberra.

Kilgour B. & Pain C. 2000. *Regolith terrains of Australia (National Geoscience Dataset)*. Geoscience Australia, Canberra.

Krieg G. W., Alexander E. M. & Rogers P. A. 1995. Eromanga Basin. *In*: Drexel J. F. & Preiss W. V. eds., *The geology of South Australia. Vol. 2, The Phanerozoic. South Australia*. Vol. **54**, pp. 101–124, Geological Survey Bulletin.

Landgrebe T. C. W. & Müller R. D. 2011. A spatio-temporal knowledge-discovery platform for Earth-Science data. *Digital Image Computing Techniques and Applications (DICTA)*. pp. 394–399. IEEE.

Langford R. P., Wilford G. E., Truswell E. M., Totterdell J. M., Yeung M., Isem A. R., Yeates A. N., Bradshaw M., Brakel A. T., Olissoff S., Cook P. J. & Strusz D. L. 1996. *Palaeogeographic atlas of Australia: time dependent summarisation of sedimentological data based on several datasets, between ~ 550 Ma to present date*. Geoscience Australia, Canberra.

Matthews K. J., Hale A. J., Gurnis M., Müller R. D. & DiCaprio L. 2011. Dynamic subsidence of Eastern Australia during the Cretaceous. *Gondwana Research* **19**, 372–383.

Minty B. R. S. 2011. Airborne geophysical mapping of the Australian continent. *Geophysics* **76**, A27–A30.

Minty B. R. S., Franklin R., Milligan P. R., Richardson L. M. & Wilford J. 2010. *Radiometric map of Australia, 2nd edition*. Geoscience Australia, Canberra.

Newberry T. L. 2004. $^{40}Ar/^{39}Ar$ Geochronology constraints on weathering profile evolution in Australian opal fields. *Australian Geological Convention*, pp. 34–34.

Norvick M. & Smith M. 2001. Southeast Australia–Mapping the plate tectonic reconstruction of southern and southeastern Australia and implications for petroleum systems. *APPEA Journal—Australian Petroleum Production and Exploration Association* **41**, 15–36.

Nykänen V., Groves D. I., Ojala V. J., Eilu P. & Gardoll S. J. 2008. Reconnaissance-scale conceptual fuzzy-logic prospectivity modelling for iron oxide copper–gold deposits in the northern Fennoscandian Shield, Finland. *Australian Journal of Earth Sciences* **55**, 25–38.

Pecover S. R. 1996. A new genetic model for the origin of opal in Cretaceous sediments of the Great Australian Basin. *Geological Society of Australia Abstracts* pp. 450–454.

Raymond O. L. & Retter A. J. 2010. *Surface geology of Australia 1:1,000,000 scale, 2010 edition (digital dataset)*. Geoscience Australia, Canberra.

Raza A., Hill K. C. & Korsch R. J. 2009. Mid-Cretaceous uplift and denudation of the Bowen and Surat Basins, eastern Australia: relationship to Tasman Sea rifting from apatite fission-track and vitrinite-reflectance data. *Australian Journal of Earth Sciences* **56**, 501–531.

Robertson R. S. & Scott D. C. 1989. *Coober Pedy Precious Stone Field [map]*. Department of Mines and Energy, South Australia, Adelaide.

Robertson R. S. & Scott D. C. 1990. *Geology of the Coober Pedy Precious Stones Field, results of investigations, 1981–86*. Energy D. o. M. a. Geological Survey of South Australia, Adelaide.

Sanders J. V. 1964. Colour of precious opal. *Nature* **204**, 1151–1153.

Senior B. R. & Chadderton L. T. 2007. Natural gamma radioactivity and exploration for precious opal in Australia. *The Australian Gemmologist* **23**, 160–176.

Senior B. R. & Mabbutt J. A. 1979. A proposed method of defining deeply weathered rock units based on regional geological mapping in southwest Queensland. *Journal of the Geological Society of Australia* **26**, 237–254.

Senior B. R., McColl D. H., Long B. E. & Whiteley R. J. 1977. The geology and magnetic characteristics of precious opal deposits, southwest Queensland. *BMR Journal of Australian Geology & Geophysics* **2**, 241–251.

Smallwood A. 1997. A new era for opal nomenclature. *The Australian Gemmologist* **19**.

Downloaded by [University of Sydney] at 15:42 05 September 2013

TAJE_A_754793.3d (TAJE) 02-05-2013 23:57

Smallwood A. G., Thomas P. S. & Ray A. S. 1997. Characterisation of sedimentary opals by Fourier transform Raman spectroscopy. *Spectrochimica Acta Part A: Molecular and Biomolecular Spectroscopy* **53**, 2341–2345.

Smallwood A. G., Thomas P. S. & Ray A. S. 2008. Characterisation of the dehydration of Australian sedimentary and volcanic precious opal by thermal methods. *Journal of Thermal Analysis and Calorimetry* **92**, 91–95.

Tan P., Steinbach M. & Kumar V. 2006. *Introduction to data mining*. Addison-Wesley, Boston, MA.

Thiry M. & Milnes A. R. 1991. Pedogenic and groundwater silcretes at Stuart Creek opal field, South Australia. *Journal of Sedimentary Research* **61**, 111–127.

Thiry M., Milnes A. R., Rayot V. & Simon-Coinçon R. 2006. Interpretation of palaeoweathering features and successive silicifications in the Tertiary regolith of inland Australia. *Journal of the Geological Society* **163**, 723–736.

Received 24 July 2012; accepted 11 November 2012

Downloaded by [University of Sydney] at 15:42 05 September 2013